Development of the TAKENAKA Multi-belled Cast-in-place Concrete Pile Method
－Bearing Capacity of Middle-belled Part of Multi-belled Pile in Sandy Ground－

Yoshio Hirai*1

Summary

The TAKENAKA multi-belled cast-in-place concrete pile method has been developed which has a shape of some bell enlargements at its axial part to improve the bearing capacity. This report describes the centrifuge model tests and in-situ pile load tests that were conducted as part of the development, and proposes a bearing capacity model of the soil under the middle-belled parts based on the experimental results, verifying the validity of the model by comparing its predictions with the experimental results. Furthermore, in comparison with the analysis model of the belled parts in previous studies, the bearing capacity of the middle-belled parts was investigated in relation to the strain level of the soil associated with the settlement of the belled parts.

Keywords: multi-belled pile, middle-belled part, bearing capacity, centrifuge model test, in-situ pile load test, sandy ground

1 Introduction

An increasingly common method for pile foundations in the construction field consists of nodular cast-in-place concrete piles (“multi-belled piles”; see Fig. 1 and Fig. 2). In this technique, a belled part is provided at a point on the axis of a cast-in-place concrete pile to improve its vertical support performance. This approach is based on the fact that taller and heavier buildings, such as high-rise offices and apartment complexes, in recent years have resulted in large loads acting on the foundations during normal times and in earthquakes. No multi-belled piles existed in Japan in the 1990s, which was when our company began developing the multi-belled pile method[1]. Internationally, only a few nodular cast-in-place piles[2] had been used in soft clayey soil, and design and construction methods had not been established. During our development, we first clarified the bearing capacity model of the soil supporting the belled part (middle-belled part) of a multi-belled pile and evaluated the bearing capacity of the belled part quantitatively.

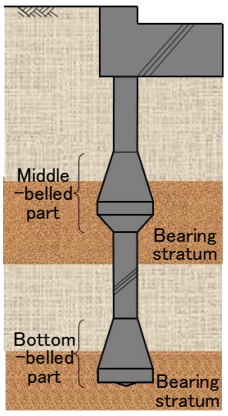

Fig.1 Multi-belled pile

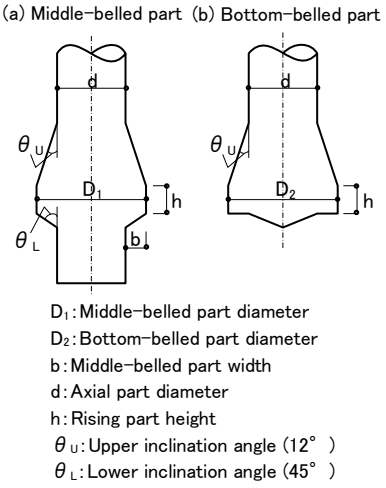

Fig.2 Middle and bottom-belled part

In this report, in Section 2, we present an overview of two types of centrifuge model tests conducted at the beginning of the development of this newly pile method and the experimental results. We then describe the observation results of the soil deformation behavior, which provided hints for clarifying the bearing capacity model of the belled part and the effect of increasing its bearing capacity. In Section 3, we present the centrifuge model test as a basis to propose a bearing capacity model (analysis model) for the soil under the bottom of the belled part while referencing previous research results. The reproducibility of the centrifuge model test results allows us to verify the validity of this analysis model. Additionally, in Section 4, we present an overview of the in-situ pile load test of a full-scale multi-belled pile and the test results. We attempt to explain the test results using the analytical model introduced in Section 3 and discuss the bearing capacity of the belled part in relation to the soil strain level associated with the penetration of this belled part. Note that some of the experimental results in this report have been published in previous papers.

2 Centrifuge model test

2.1 Experimental overview

We conducted two types of model experiments[3] (“Experiment A” and “Experiment B”) using a centrifuge loading test

＊1 Senior Chief Researcher, Research & Development Institute, Dr. Eng.

apparatus. We present an overview of each experiment below. For Experiment A, we conducted a model pile loading test on a multi-belled pile and a pile with a widened base in a centrifugal field of 80G (G: gravitational acceleration) to understand the bearing capacity of the middle-belled part of the multi-belled pile. Fig. 3 shows an overview of the loading device of the model pile mounted on the centrifuge loading test apparatus (a beam-type loading device with an effective rotation radius of 6.5 m; see Photo 1). The dimension of the model pile tip was 290 mm, whereas that of the middle-belled part was 245 mm. The pile head of the model pile was free before being loaded so that the model pile could follow the settlement of the model soil that occurred before reaching a specified centrifugal field. Fig. 4(a) and Table 1 present the specifications of the model pile (the symbols in Fig. 4 are included in Table 1). The lower inclination angle of the middle-belled part of the model pile was 45°. Table 2 presents the physical and mechanical properties of the Toyoura sand used in the model soil in an air-dried state. We used the air-drop method to create the model soil. The relative density (Dr) of the model soil measured using a constant volume container was approximately 90%. Table 2 also lists the results of a consolidated drained triaxial compression test (CD test) of Toyoura sand (Dr = 90%). The experimental method used was unidirectional loading with a displacement control method at a loading rate of 0.5 mm/min. The measurement items were the load of the pile head measured by a load cell and the settlement measured by a displacement meter.

Meanwhile, for Experiment B, we loaded a half-split multi-belled pile into the model soil in a centrifugal field (40G) and visually observed the soil behavior around the pile to understand the soil behavior near the middle-belled part during loading. Fig. 4(b) and Table 1 present the specifications of the model pile. We used the same experimental apparatus utilized in Experiment A and created the model soil in the same way. One side of the experimental soil tank was made of a transparent acrylic board, and the movement of the colored sand (colored Toyoura sand) that had been spread horizontally in advance was observed through the acrylic board by loading the half-split model pile along the acrylic board. In Experiment B, we changed the model pile specifications from those used in Experiment A to facilitate visual observation of the behavior of the soil around the pile.

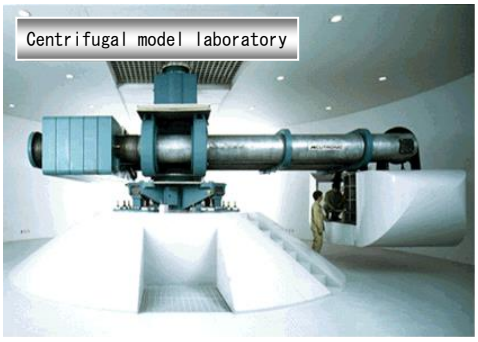

Photo 1 Centrifuge loading test apparatus

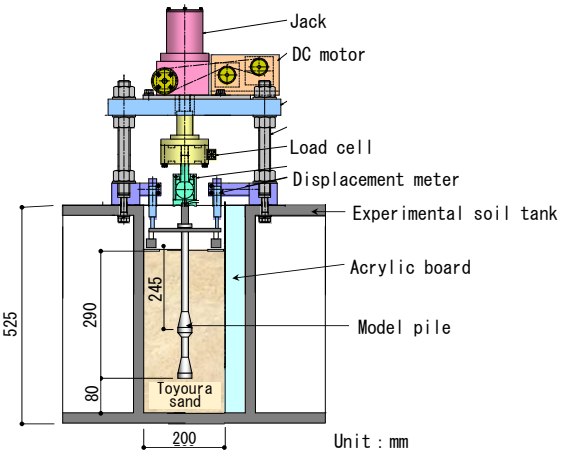

Fig.3 Model pile loading device

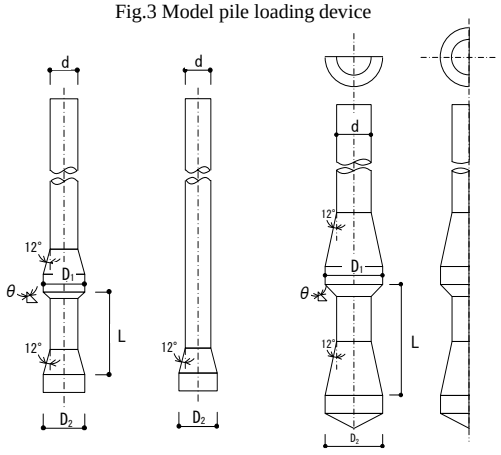

(a) Model pile: Experiment A (b) Half-sprit model pile: Experiment B

Fig.4 Model pile

Table 1 Model pile specification (model dimensions)

Experi-ment	Pile shape	Axis part diameter d(mm)	Middle-belled part diameter D_1(mm)	Bottom-belled part diameter D_2(mm)	Belled part interval L(mm)	Middle-belled part lower inclination angle θ(°)
A	Multi-belled pile	12.5	17.5	17.5	35.0	45.0
	Belled pile	12.5	—	17.5	—	—
B	Half-split multi-belled pile	25.0	45.0	45.0	90.0	45.0

*Model pile material: High-strength aluminum (Young's modulus: approx. 70 GPa)

Table 2 Physical/mechanical properties of Toyoura sand

50% particle size D_{50}(mm)	Uniformity factor Uc	Density ρ_d(kN/m³)		Adhesive force c'(kN/m²)	Internal friction angle φ'(°)
		Maximum	Minimum		
0.187	1.62	16.26	13.40	31.7	40.9

2.2 Experimental results

[Experiment A results]

Fig. 5 shows the relationship between the load at the pile head of the multi-belled and bottom-belled piles

("pile head load") and the settlement ratio δ/D_2 (δ: settlement, D_2: bottom-belled part diameter). The vertical axis of the figure is the measured pile head load converted to the actual value. Owing to the mechanism of the loading device, the maximum pile head load was 10 mm for the model dimensions, and the maximum value of δ/D_2 was 0.57 for both piles. The figure shows the results of three experiments, and the pile head load increased monotonically with increasing settlement ratio. The pile head load of the multi-belled pile was also larger than that of the bottom-belled pile with the same settlement ratio. Based on the experimental results, we estimated the ultimate bearing capacity of the middle-belled part of the multi-belled pile by assuming that the load difference between the pile head load (mean value) of the multi-belled pile and that of the bottom-belled pile was the bearing capacity of the middle-belled part and by calculating the relationship between the bearing capacity of the middle-belled part and the settlement ratio (red solid line in Fig. 5). The bearing capacity of the middle-belled part increased with increasing settlement ratio but reached an upper limit at approximately $\delta/D_2 = 0.4$ and subsequently remained almost constant, suggesting that the bearing capacity reached an ultimate limit. A separately conducted centrifugal model pile pull-out experiment[4] confirmed that the above assumption did not overestimate the bearing capacity of the middle-belled part given the relatively small shaft resistance force of the pile axis (mean value: approximately 23 kN/m^2).

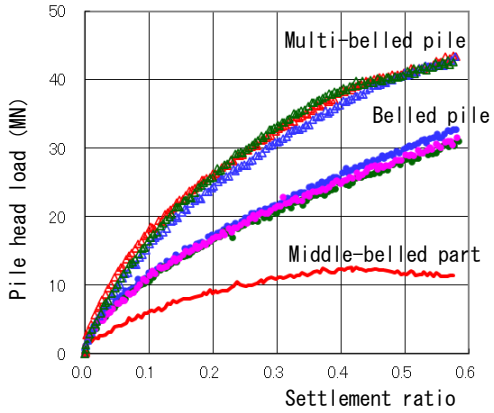

Fig.5 Relation between pile head load and settlement ratio

The mean pile head loads at $\delta/D_2 = 0.57$ were 43.2 and 31.8 MN, respectively, and the load difference was 11.4 MN (maximum value: 12.6 MN). If we assume that the maximum value of this load difference is the ultimate bearing capacity of the middle-belled part, then we can calculate the ultimate bearing capacity degree qm of the middle-belled part (bearing capacity degree of the ring surface of the horizontal projection of the middle-belled part excluding the axis part) as qm = 16,700 kN/m^2. The bearing capacity of the middle-belled part at a settlement ratio $\delta/D_2 = 0.1$, which is the guideline for settlement when examining the ultimate bearing capacity of piles in practical design, is 5.9 MN, and the bearing capacity degree of the middle-belled part at this time is qm = 7,800 kN/m^2.

[Experiment B results]

Photos 2(a) and (b) show the state of soil displacement near the pile when a half-split model pile was loaded into the model soil at $\delta/D_2 = 0.1$ and 0.4, respectively. The black outline drawn on the acrylic board indicates the initial position of the pile. The observation results of the displacement behavior of the colored sand shown in Photo 2 showed that the soil directly below the middle-belled part was loaded vertically and spread horizontally as the pile settled. In particular, at $\delta/D_2 = 0.4$ (Photo 2(b)), the middle-belled part exhibited the appearance of punching shear failure, as it was loaded through the soil along the slip line that appeared diagonally downward from its bottom end. Visual observations also showed that the vertical influence range of the soil that contributed to the bearing capacity of the middle-belled part at $\delta/D_2 = 0.1$ was approximately $1 \cdot D_1$ (D_1: middle-belled part diameter) vertically downward from the bottom end of its rising part.

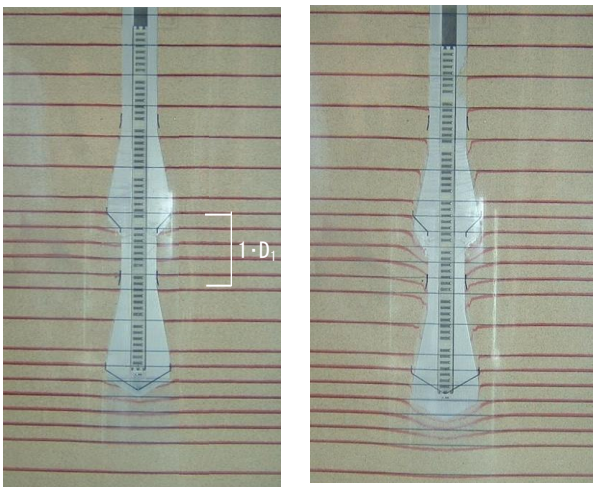

(a) $\delta/D_2=0.1$ (b) $\delta/D_2=0.4$

Photo 2 Soil behavior around model pile

3 Bearing capacity model of middle-belled part

3.1 Previous research

The main previous studies on the bearing capacity model of the belled part installed at a pile axis are those by Ishidou[5),6)], Ogura et al.[7)], and Yao et al.[8)]. These theoretical or experimental studies applied the bearing capacity theory proposed to clarify the bearing capacity model of the pile-tip soil to the belled part to examine the bearing capacity model of the belled part.

Ishidou was the first in Japan to theoretically address the bearing capacity model of the nodular pile. It discussed the ultimate bearing capacity of the bottom of the belled part using the Prandtl-based bearing capacity theory based on 2D rigid plasticity theory. Ogura et al. used model experiments with an experimental tank as a basis to consider the bearing capacity of the belled part as a shear resistance force acting on a cylindrical shear surface with a diameter slightly larger than the diameter of the belled part in the soil around the pile below the bottom of the belled part and examined the bearing capacity of the entire nodular pile. Yao et al. also used the ultimate bearing capacity equation for the bottom surface of the belled part derived by Ishidou as a basis for deriving an equation for calculating the bearing capacity for axisymmetric problems. Here, we used the centrifuge model test shown in Section 2 as a basis to quantitatively evaluate the bearing capacity of the bottom of the belled part calculated from the bearing capacity equation proposed by Ishidou and discussed the validity of the proposed bearing capacity model. Next, we applied the bearing capacity theory proposed by Takano and Kishida[9)], which combines the Prandtl-based bearing capacity theory with the cylindrical cavity expansion theory for the bearing capacity model of the pile-tip soil, to the bearing capacity model of the belled part. We then compared these results with the centrifuge model test results to discuss the applicability of this bearing capacity theory.

3.2 Research by Ishidou

Ishidou assumed that the belled part was a type of 2D strip foundation, as shown in Fig. 6, and derived the bearing capacity equation for the belled part from the balance of forces. This equation considered the wedge zone acting mainly on the soil below the bottom of the belled part and the plastic zone, which is assumed to be a logarithmic spiral sliding surface. The research assumed that the effective overburden pressure at the depth of the bottom of the belled part in the soil is σ_v' and that the 2D Rankine passive earth pressure is the horizontal stress acting on the vertical plane AD directly below the belled part in the ultimate state. Assuming that the ultimate bearing capacity of the bottom of the belled part is Q_L and the degree of ultimate bearing capacity is q_L (= Q_L /b, b: protruding width of the belled part), q_L was given by the following equation:

$$q_L = Q_L/b = c \cdot N'_c + \gamma' \cdot z \cdot N'_q \quad (1)$$

$$N'_c = 2\sqrt{K_p} \cdot \cos(\alpha - \phi_s)/(\cos\phi_s \cdot \cos\alpha) \cdot \exp\{2(\pi/2 - \alpha)\tan\phi_s\}$$

$$N'_q = \sqrt{K_p}/2 \cdot N'_c$$

$$K_p = \tan^2(\pi/4 + \phi_s/2)$$

Where c: soil adhesion, ϕ_s: soil internal friction angle,
α: main working wedge base angle,
γ': soil effective unit volume weight,
z: belled part base depth,
K_p: Rankine passive earth pressure coefficient, and
N_c', N_q': bearing capacity coefficient.

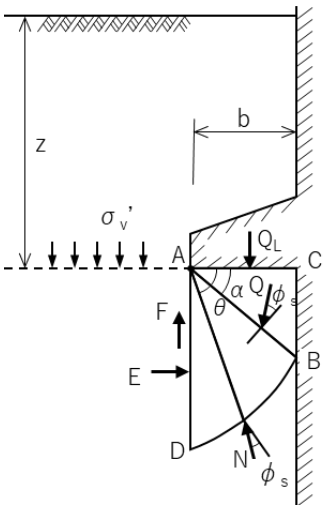

Fig.6 Analysis model of ultimate bearing capacity (Ishidou[5) ,6)])

We evaluated the ultimate bearing capacity of the belled part in the centrifugal model pile experiment described in Section 2 using Ishidou's proposed equation. We set the soil constants and other variables to specifically calculate the ultimate bearing capacity of the belled part. For the centrifuge model test, we used air-dried Toyoura sand as the experimental soil. The results of the consolidated drainage triaxial compression test of Toyoura sand with the same relative density as that in the experiment were c = 31.7 kN/m^2 and φ_s = 40.9°. The effective overburden pressure at the bottom depth of the belled part (model dimension of the embedded depth: 245 mm) was σ_v' = 16 kN/m^3 × 19.6 m = 314 kN/m^2, and the Rankine passive earth pressure coefficient was K_p = 4.8. Calculating the ultimate bearing capacity of the belled part using these soil constants yielded a value of q_L = 10,000 kN/m^2 (bearing capacity coefficients: N_c' = 27, N_q' = 29). This analytical value was equivalent to approximately 60% of the ultimate bearing capacity of the belled part

(16,700 kN/m^2), estimated based on the centrifuge model test results, and was considerably smaller than the experimental value. The discrepancy between the analytical and experimental values was thought to be due to the difference in the strain level of the soil due to the penetration of the belled part examined in this study. In other words, the analytical value based on Ishidou's proposed equation gave the ultimate bearing capacity when the penetration of the belled part was relatively small and the soil below the base of the belled part was partially plastic (equivalent to the first ultimate bearing capacity defined by Takano[10] for the soil at the tip of the pile). Meanwhile, the experimental value obtained from the centrifuge model test was thought to be the ultimate bearing capacity when the belled part was further penetrated into the soil and was thought to be the maximum bearing capacity that the soil below the base of the belled part can ultimately exert (second ultimate bearing capacity defined by Takano[10] for the soil at the tip of the pile). Incidentally, the settlement ratio δ/D_2 at which the bearing capacity of the belled part obtained from the centrifuge model test was equal to Ishidou's analytical value of the ultimate bearing capacity q_L = 10,000 kN/m^2 was approximately 0.14. This suggests that the bearing capacity of the belled part reached the first ultimate bearing capacity at a settlement ratio of approximately 0.14 in the centrifuge model test.

In the next section, we sought to reproduce the bearing capacity in the extreme state (second ultimate bearing capacity) that can be estimated from the centrifuge model test results by discussing the failure mechanism of the soil below the bottom of the belled part, with reference to the research results of Takano and Kishida.

3.3 Research by Kishida and Takano

Takano and Kishida[9] conducted a model pile experiment that could reproduce the same stress state as that near the tip of an actual pile by applying pressure to the model soil. They used their obtained observation results to propose a bearing capacity theory for the pile-tip soil that combines the Prandtl bearing capacity equation and that based on the cylindrical cavity expansion theory. Fig. 7 shows the analytical model of the ultimate bearing capacity of the pile-tip soil proposed by Takano[10]. The main wedge △ABC was formed in the soil under the pile base, and transition regions BCD and ACD' were assumed on both sides. The observation results of the soil movement in the model pile experiment showed that the soil outside the BD and AD' planes was pushed aside as the pile penetrated. This suggested that the soil failure mechanism that expands the cylindrical cavity was close to the actual phenomenon, and we assumed that the boundary stress at the limit on the BD and AD' planes was equal to the ultimate internal pressure when the cylindrical cavity was expanded.

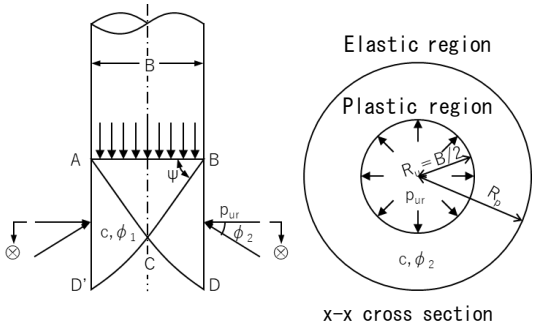

Fig.7 Analysis model of ultimate bearing capacity (Takano[10])

The observation results of the behavior of the soil under the bottom of the middle-belled part in the centrifuge model test (Experiment B) for the multi-belled pile shown in Section 2 also showed that the soil directly below the middle-belled part was loaded vertically and also spread horizontally as the pile penetrated. Thus, the analytical model for the ultimate bearing capacity of the soil at the pile tip proposed by Takano was applied to the study of the bearing capacity model for the bottom of the middle-belled part. Fig. 8 shows the proposed analytical model of the ultimate bearing capacity of the soil under the bottom of the middle-belled part. As with the soil at the pile tip, we assumed that a main wedge was formed in the soil below the bottom of the middle-belled part, and a logarithmic spiral transition region occurred on the sliding surface. In the ultimate state, the ultimate internal pressure was set as acting on the BD surface below the bottom of the middle-belled part when the cylindrical cavity was expanded. We then determined the ultimate bearing capacity equation for the bottom of the middle-belled part. If the shear strength of the soil in the plastic region is determined by the Mohr–Coulomb failure criterion,

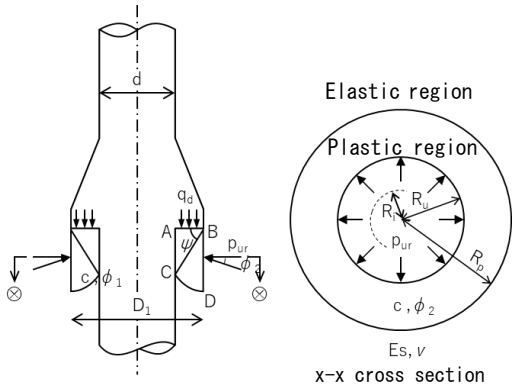

Fig.8 Analysis model of ultimate bearing capacity (Middle-belled part)

then the ultimate internal pressure p_{ur} when the cylindrical cavity is expanded is given by the following equation:

$$p_{ur} = c F_{c2} + p_m F_{q2} \quad (2)$$

$$F_{c2} = \{(1+\sin\phi_2)\cdot I_c^{\sin\phi_2/(1+\sin\phi_2)} - 1\}\cdot\cot\phi_2$$

$$F_{q2} = 3(1+\sin\phi_2)/\{2(1+\nu)\}\cdot I_c^{\sin\phi_2/(1+\sin\phi_2)}$$

$$I_c = E_s/[2(1+\nu)\{c+3/\{2(1+\nu)\}\cdot\tan\phi_2\cdot p_m\}\cdot\cos\phi_2]$$

Where c: soil cohesion, ϕ_2: soil internal friction angle (within the plastic region of cylindrical shape),

p_m: mean principal stress at the bottom depth of the middle-belled part, ν: Poisson's ratio of soil,

Es: soil deformation coefficient, and

F_{c2}, F_{q2}: cylindrical cavity expansion coefficient.

Next, we determined the relationship between the ultimate internal pressure p_{ur} acting on the BD surface and the ultimate bearing capacity q_d of the middle-belled part. In this study, we examined a case where the effective overburden pressure at the bottom depth of the middle-belled part is sufficiently large. Therefore, we ignored the weight of the soil in the sliding area and assumed that the soil was a rigid-plastic body. In 2D analysis, q_d is given by the following equation:

$$q_d = c F_{c1} + p_{ur} F_{q1} \quad (3)$$

$$F_{c1} = (\cot\phi_1+\tan\psi)\, e^{(\pi-2\psi)\tan\phi_1} - \cot\phi_1$$

$$F_{q1} = (1+\tan\phi_1\cdot\tan\psi)\, e^{(\pi-2\psi)\tan\phi_1}$$

Where c: soil cohesion,

ϕ_1: soil internal friction angle (main wedge under the bottom of the belled part and soil in the transition region),

Ψ: base angle of the main wedge[11] (assuming that the bottom of the belled part is rough, $\Psi=\pi/4+\phi_1/2$), and

F_{c1}, F_{q1}: bearing capacity coefficient.

Assuming from Eqs. (2) and (3) that the internal friction angle of the soil under the bottom of the middle-belled part is uniform ($\phi_1=\phi_2=\phi$), then the ultimate bearing capacity degree q_d of the middle-belled part is given by the following equation:

$$q_d = c N_c + p_m N_q \quad (4)$$

$$N_c = (1+\tan\phi\cdot\tan\psi)\, e^{(\pi-2\psi)\tan\phi}\{(1+\sin\phi)\cdot I_c^{\sin\phi/(1+\sin\phi)} - 1\}\cdot\cot\phi + (\cot\phi+\tan\psi)\, e^{(\pi-2\psi)\tan\phi} - \cot\phi$$

$$N_q = (1+\tan\phi\cdot\tan\psi)\, e^{(\pi-2\psi)\tan\phi}\cdot 3(1+\sin\phi)/\{2(1+\nu)\}\cdot I_c^{\sin\phi/(1+\sin\phi)}$$

$$I_c = E_s/[2(1+\nu)\{c+3/\{2(1+\nu)\}\cdot\tan\phi\cdot p_m\}\cdot\cos\phi]$$

Where c: soil cohesion, ϕ: soil internal friction angle,

Ψ: base angle of main wedge (assuming that the base of the middle-belled part is rough, $\Psi=\pi/4+\phi/2$),

p_m: mean principal stress at the bottom of the middle-belled part, ν: soil Poisson's ratio,

Es: soil deformation coefficient, and N_c, N_q: bearing capacity coefficient.

We used Eq. (4) to evaluate the ultimate bearing capacity of the middle-belled part in the centrifuge model test described in Section 2. We set the soil constants to specifically calculate the ultimate bearing capacity of the middle-belled part. For the centrifuge model test, the results of the consolidated drainage triaxial compression test of Toyoura sand used as the experimental soil were c = 31.7 kN/m^2 and ϕ = 40.9°. The mean principal stress at the bottom of the middle-belled part can be calculated from $p_m = (1 + 2K)\cdot p_v/3$, where K is the soil lateral pressure coefficient, and p_v is the effective overburden pressure at the bottom depth of the middle-belled part. For the lateral pressure coefficient in the plastic region of the pile shaft soil, we referenced the K value for embedded piles in the evaluation of the pile-tip bearing capacity based on the spherical cavity expansion theory by Yamaguchi[12] and assumed K = 0.5. At the bottom depth of the middle-belled part, the effective overburden pressure was p_v = 314 kN/m^2 and the mean principal stress was p_m = 209 kN/m^2. When calculating the ultimate internal pressure p_{ur} in the theory of cylindrical cavity expansion, we assumed that the soil outside the plastic region under the bottom of the middle-belled part was an isotropic elastic body with a deformation coefficient Es and a Poisson's ratio ν. Further, we assumed that the volume change when the cylindrical cavity was expanded from the initial radius Ri to the inner radius Ru at the ultimate internal pressure was equivalent to the volume change due to the displacement of the elastic–plastic boundary. Therefore, the setting of the deformation coefficient and Poisson's ratio in the elastic region was also important in estimating the ultimate internal pressure (see Fig. 8). Here, we used the results of a pressuremeter test that reproduced the soil behavior in a cylindrical cavity expansion state in a laboratory triaxial cell as a basis to set the deformation coefficient in the elastic region of the soil. Fukagawa[13] analyzed the

stress level dependence of the deformation coefficient from the relationship between the deformation coefficient and consolidation pressure obtained from a miniature pressuremeter test on Toyoura sand. Based on these results, the deformation coefficient during the initial loading process is approximately Es = 2.0 × 10^4 kN/m^2 when the consolidation pressure (mean principal stress) is approximately 200 kN/m^2, and therefore we adopted this value. We also assumed the Poisson's ratio to be ν = 0.3. The soil constants set in this manner were used to calculate the ultimate bearing capacity q_d of the middle-belled part, which yielded a value of q_d = 13,000 kN/m^2 (bearing capacity coefficients: N_c = 53, N_q = 54). This analytical value corresponded to approximately 78% of the ultimate bearing capacity of the middle-belled part (16,700 kN/m^2) estimated based on the centrifuge model test results. Although the analytical result was slightly smaller than the experimental value, the results suggested that the centrifuge model test results could be quantitatively reproduced. Together with the observation results of the behavior of the soil under the bottom of the middle-belled part in the centrifuge model test (Experiment B), this analytical result shows the validity of applying the bearing capacity theory, which combines the Prandtl-based bearing capacity equation and the cylindrical cavity expansion theory, to the bearing capacity model in the region where the strain level of the soil at the bottom of the middle-belled part is large.

4 In-situ pile load test

4.1 Test overview

In a project in which a multi-belled pile was adopted[14], an in-situ pile load test[15] was implemented on a full-scale pile to confirm the bearing capacity of the middle-belled part anchored in the gravel soil. Here, we present an overview of the load test and the test results. We applied the equation proposed by Ishidou, shown in Section 3, and the bearing capacity theory combining the Prandtl bearing capacity equation and the cylindrical cavity expansion theory to the interpretation of the in-situ pile load test results. On this basis, we discuss the bearing capacity model of the soil below the bottom of the middle-belled part.

Fig. 9 shows an overview of the test pile and soil, and Table 3 lists the pile specifications. The test pile was a multi-belled pile made of high-strength concrete (Fc60 N/mm^2) with an axis diameter of 1.2 m, a middle-belled part diameter of 1.6 m, and a pile-tip depth of 86.7 m. The middle-belled part of the test pile was fixed in a gravel layer at a depth of GL−50 to −60 m, and the tip was fixed in a fine sand layer at a depth of ≥80 m. The test pile was friction-cut by using double steel pipes from the soil GL to GL−39 m.

We based the loading test method on the Japanese Geotechnical Society standard and used a multi-cycle step loading method with 6 cycles and 21 steps (maximum jack load: 42 MN). The load was measured using the pressure transducer of a hydraulic jack, and the vertical displacements of the pile head, middle-belled part, and tip of the test pile were measured using a double pipe installed inside the pile body. We also estimated the axial force at the pile body cross section by measuring the rebar strain at eight cross sections in the depth direction ((1)–(8) in Fig. 9(b)) and the steel pipe strain at two cross sections in the depth direction ((1)–(2)).

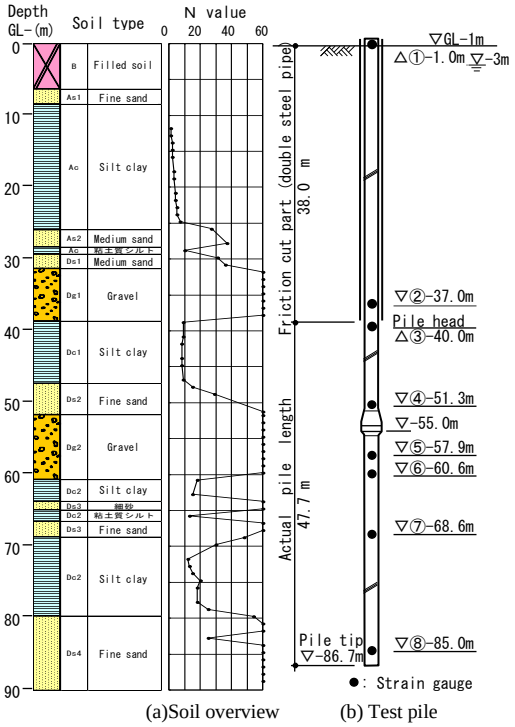

Fig.9 Loading test pile and ground profile

Table 3 Loading test pile specification

Pile Name	Axial part diameter (m)	Middle-belled part diameter (m)	Bottom-belled part diameter (m)	Actual pile length (m)	Pile tip depth (m)	Pile number	Construction method
Test pile	1.2	1.6	1.2	47.7	86.7	1	Earth drill method
Reaction pile	1.6	—	2.2	37.6	38.6	4	

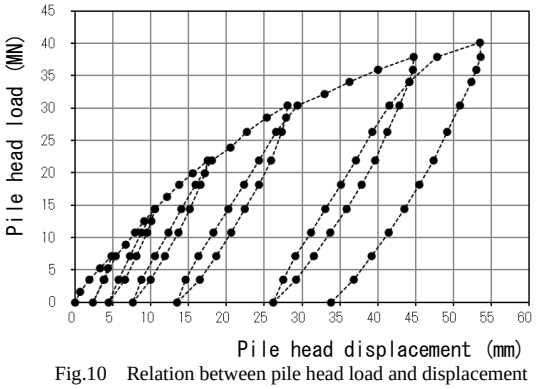

Fig.10 Relation between pile head load and displacement

4.2 Test results

Fig. 10 shows the relationship between the load and displacement at the pile head ((3) GL−40 m below the friction cut). A displacement of 54 mm occurred at the maximum load of 40.1 MN. Fig. 11 shows the depth distribution of the rebar strain and steel pipe strain. Please refer to reference[15] for the method of estimating the axial force at each measurement section. Fig. 12(a) and (b) show the depth distribution of the pile axial force and shaft resistance force (hereinafter, τ), respectively. The τ value was calculated by dividing the axial force difference in the measurement section by the shaft area of the axis. Fig. 12(a) shows that there is a large axial force difference in sections (4)–(5), which include the middle-belled part, and the maximum value of τ was 567 kN/m^2. Fig. 13 presents the relationship between τ and the amount of displacement. We calculated the relative displacement between the pile and soil by subtracting the mean contraction of each section based on the rebar strain from the displacement of the pile head. The figure shows that τ in the axis reached its upper limit at a displacement of approximately 10–20 mm and became almost constant, whereas τ in sections (4)–(5), which included the middle-belled part, and sections (5)–(6) of the axis directly below the middle-belled part tended to increase with increasing displacement. This tendency of the middle-belled part was also observed in the centrifuge model test results, and the resistance mechanism in sections (4)–(5), which included the middle-belled part, was considered a bearing capacity model. Sections (5)–(6) of the axis directly below the middle-belled part also exhibited a similar tendency. This result was attributed to the fact that the middle-belled part pressed down the soil below the bottom, which increased the confining pressure of the shaft soil. This in turn resulted in the shaft resistance force increasing with increasing displacement. Fig. 13 shows a curve estimated by fitting the Weibull distribution from the relationship between τ and displacement in sections (4)–(5), which included the middle-belled part. If τ at a displacement of 160 mm (settlement ratio 0.1), which corresponds to 10% of the middle-belled part diameter, is taken as the limit value τ_u, then τ_u = 680 kN/m^2.

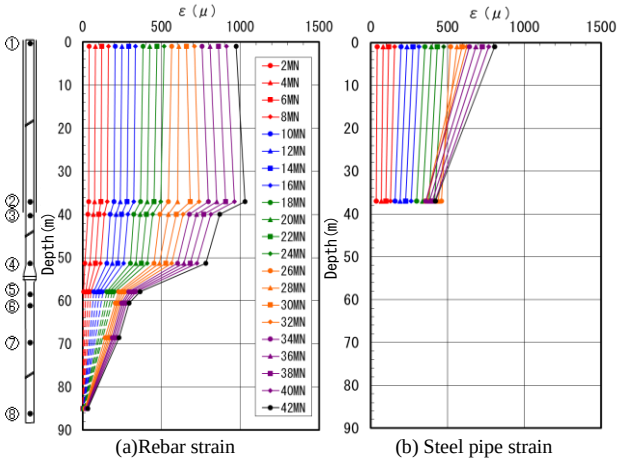

(a)Rebar strain (b) Steel pipe strain

Fig.11 Strain distribution of reinforcement and steel pipe in depth

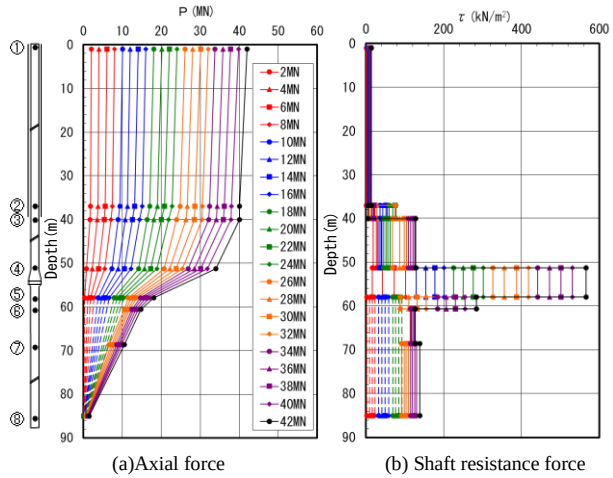

(a)Axial force (b) Shaft resistance force

Fig.12 Depth distribution of axial force and shaft resistance force

4.3 Discussion of bearing capacity of middle-belled part

We discuss the ultimate bearing capacity of the middle-belled part at a settlement ratio of 0.1 estimated from the in-situ pile load test of the multi-belled pile by applying Ishidou's proposed equation and a bearing capacity equation that combines the Prandtl-based bearing capacity theory and the cylindrical cavity expansion theory.

The ultimate bearing capacity qm of the middle-belled part based on the in-situ pile load test results was calculated from the following equation:

$q_m = P_m / A_m$

P_m: Ultimate resistance of the middle-belled part (=P④-⑤-R_1-R_2-R_3),

P④-⑤: Axial force difference between sections (4)–(5) (calculated from τ_u)

R_1,R_2,R_3: Resistance of axis part and rising part in sections (4)–(5), and

A_m: Horizontal projection area of the ring (=0.88 m^2).

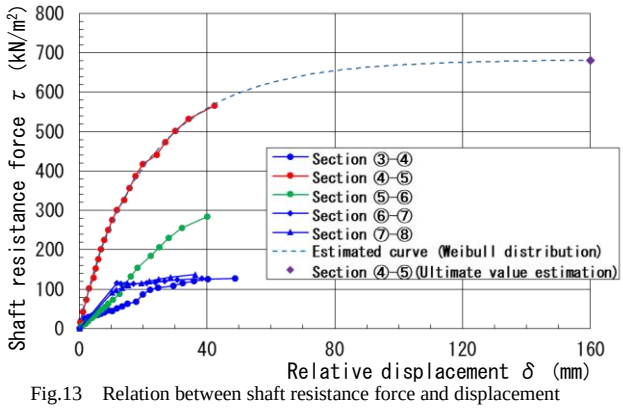

Fig.13 Relation between shaft resistance force and displacement

Given that Pm = 11,400 kN and Am = 0.88 m^2, the ultimate bearing capacity of the middle-belled part is q_m = 13,000 kN/m^2.

We evaluated the ultimate bearing capacity of the middle-belled part using Ishidou's proposed equation. The middle-belled part was anchored in the alluvial gravel layer (thickness: 9.0 m, mean converted N value: 100) deposited at GL−51.6 to −60.6 m (anchored depth: GL−55.0 m, see Fig. 9). No mechanical tests have been conducted on the alluvial gravel layer, so the internal friction angle ϕ_d of the gravel was estimated based on the converted N value, with consideration given to its confining pressure dependence[16] (ϕ_d = 40°). The effective overburden pressure at the bottom depth of the rising part of the middle-belled part is σ_v' = 405 kN/m^2, and the Rankine passive earth pressure coefficient K_p = 4.6. We used these soil constants to calculate the ultimate bearing capacity q_L of the middle-belled part as q_L = 10,900 kN/m^2 (assuming bearing capacity coefficients N_c' = 25, N_q' = 27, and c = 0 kN/m^2). This analytical value corresponds to approximately 84% of the ultimate bearing capacity of the middle-belled part (q_m = 13,000 kN/m^2) estimated from the in-situ pile load test results and is slightly smaller than the test results. Meanwhile, we evaluated the ultimate bearing capacity of the middle-belled part by applying the bearing capacity theory, which combines the Prandtl bearing capacity equation and the cylindrical cavity expansion theory. We used the above-mentioned setting basis to set the internal friction angle of the gravel that is fixed in the middle-belled part to ϕ = 40° (assuming cohesion c = 0 kN/m^2). The mean principal stress at the bottom end depth of the rising part of the middle-belled part, which corresponds to the bottom depth of the middle-belled part, was calculated from $p_m = (1 + 2K) \cdot p_v /3$ (K: soil lateral pressure coefficient, pv: effective overburden pressure at the bottom depth of the middle-belled part). The lateral pressure coefficient of the ultimate state in the cylindrical plastic region of the pile shaft soil is K = 0.5. Based on Yamaguchi's assumption, the effective overburden pressure at the bottom depth of the middle-belled part is p_v = 405 kN/m^2, and the mean principal stress is p_m = 270 kN/m^2. The deformation coefficient Es for calculating the ultimate internal pressure pur in the cylindrical cavity expansion theory was set as follows. Tsuchiya and Toyooka[17] classified the relationship between the deformation coefficient Es obtained from the borehole horizontal loading test (pressuremeter test) and the converted N value obtained from the standard penetration test by classifying them by soil type and organizing the correlation. The correlation between the Es and N values in diluvial gravel layers exhibits some variation, but the deformation coefficient is approximately Es = 4.0 × 10^4 kN/m^2 when the converted N value = 100 (Poisson's ratio is assumed to be ν = 0.3). Calculating the ultimate bearing capacity degree qd of the middle-belled part using the soil constants set in this manner yields q_d = 16,300 kN/m^2 (bearing capacity coefficient: N_c = 61, N_q = 60). This analytical value is equivalent to approximately 125% of the ultimate bearing capacity (q_m = 13,000 kN/m^2) of the middle-belled part estimated from the in-situ pile load test results, resulting in a slightly larger analytical value.

The ultimate bearing capacity of the middle-belled part (q_m = 13,000 kN/m^2) estimated from the in-situ pile load test results corresponds to the bearing capacity when the settlement ratio δ/D_1 (δ: middle-belled part settlement, D_1: middle-belled part diameter) is δ/D_1 = 0.1. This ultimate bearing capacity value is intermediate between the ultimate bearing capacity of the middle-belled part calculated using Ishidou's proposed equation (q_L = 10,900 kN/m^2) and that calculated using a bearing capacity theory that combines the Prandtl series bearing capacity equation and cylindrical cavity expansion theory (q_d = 16,300 kN/m^2). This suggests that the bearing capacity model of the soil under the bottom of the middle-belled part when the settlement ratio δ/D_1 = 0.1 in the in-situ pile load test is in the process of transitioning from a partially plasticized state to a state in which the maximum bearing capacity is finally exerted as settlement progresses.

5 Conclusion

In this study, we examined the bearing capacity model of the middle-belled part (belled part) of a multi-belled pile in sandy ground. Specifically, we presented Ishidou's bearing capacity theory, which is a representative example in previous research. We also proposed an analytical model of the bearing capacity of the soil under the bottom of the middle-belled part based on the centrifuge model test and the research results of Takano and Kishida and verified the validity of this analytical model from the reproducibility of the experimental results. Furthermore, we attempted to explain the results of a full-scale in-situ pile load test using the analytical model and discussed the bearing capacity exerted by the middle-belled part in relation to the strain level of the soil caused by the penetration of the middle-belled part. The ultimate bearing capacity calculated from Ishidou's bearing capacity equation has the limit value in the region where the settlement ratio of the middle-belled part is relatively small (corresponding to the first ultimate bearing capacity defined by Takano). Meanwhile, the ultimate bearing capacity calculated

from the proposed bearing capacity theory combining the Prandtl-based bearing capacity theory with the cylindrical cavity expansion theory has the limit value in the region where the settlement ratio is large (corresponding to the second ultimate bearing capacity defined by Takano).

6 Acknowledgements

We would like to express our sincere gratitude to Mr. Shuichi Wakai, Mr. Masamichi Aoki, and other related parties who worked with us on this development, as well as to the former trainees at the Takenaka Research & Development Institute who cooperated with the experiments and other aspects of this study.

References

1) Hirai, Y., Wakai, S., Aoki, M.: "Development of multi-belled cast-in-place concrete pile construction method", AIJ Journal of Technology and Design, Vol. 14, No. 28, pp. 433-438, October 2008.

2) Mohan, D. and Jain,G.S. : Bearing Capacity of Bored Piles in Expansive Clays, Proc. of 5th ICSMFE, Vol.2, pp.117-121, 1961.

3) Hirai, Y., Wakai, S., Aoki, M.: "Bearing capacity of middle-belled part of multi-belled pile in sand (part 1): Centrifuge model test", Summaries of Technical Papers of the Annual Meeting of the Architectural Institute of Japan B-1, pp. 361-362, July 2011.

4) Hirai, Y., Wakai, S., Aoki, M.: "Centrifuge model tests on uplift resistance of belled pile in sand", Journal of Structural and Construction Engineering (Transactions of AIJ), Vol. 74, No. 643, pp. 1613-1619, September 2009.

5) Ishidou, M.: "Bearing capacity of ledge pile in sand", Bulletin of the Faculty of Engineering Kyushu Sangyo University, No. 6, pp. 40–50, June 1970.

6) Ishidou, M.: "Bearing capacity of ledge piles in cohesive soils", Bulletin of the Faculty of Engineering Kyushu Sangyo University, No. 8, pp. 12–40, June 1971.

7) Ogura, H., Yamagata, K., Kishida, H.: "Study on bearing capacity of nodular cylindrical pile by scaled model test", Journal of Structural and Construction Engineering (Transactions of AIJ), Vol. 374, pp. 87–97, April 1987.

8) Yao, S., Ito, A., Masui, T., Ito, H.: "Bearing capacity formulae for nodal base of nodular cast-in-place concrete pile", Journal of Structural and Construction Engineering (Transactions of AIJ), Vol. 67, No. 556, pp. 79–84, June 2002.

9) Takano, A., Kishida, H.: "Failure mechanism of soil mass under base of non-displacement pile in sand", Transactions of the Architectural Institute of Japan, Vol. 285, pp. 51–62, November 1979.

10) Takano, A.: "Base resistance of non-displacement pile in sands", Doctoral dissertation, Tokyo Institute of Technology, March 1981.

11) Yamaguchi, H., Kimura, T., Fujii, N.: "Experimental studies on the bearing capacity of shallow foundations by the use of a centrifuge", Proceedings of the Japan Society of Civil Engineers, No. 233, pp. 71–85, January 1975.

12) Yamaguchi, H.: "Research on end bearing capacity of pile by elastoplastic analysis", Technical Report of the Department of Civil Engineering, Tokyo Institute of Technology, No. 16, July 1974.

13) Fukagawa, R.: "Research on estimation of deformation and strength constants of soil by pressuremeter tests", Doctoral dissertation, Kyoto University, February 1986.

14) Awano, M., Yoshida, S., Okahashi, M., Hirai, Y., Wakai, S.: "Design and construction example of super-high rise building using multi-belled pile method", Foundation Engineering & Equipment, Monthly, Vol. 42, No. 2, pp. 33–36, February 2014.

15) Wakai, S., Onishi, N., Hirai, Y., Aoki, M.: "In-situ load test for multi-belled cast-in-place concrete pile (Part 1), (Part 2)", Summaries of Technical Papers of the Annual Meeting of the Architectural Institute of Japan B-1, pp. 441-444, September 2015.

16) Hatanaka, M., Uchida, A., Kakurai, M., Aoki, M.: "A consideration on the relationship between SPT N-value and internal friction angle of sandy soils", Journal of Structural and Construction Engineering (Transactions of AIJ), Vol. 63, No. 506, pp. 125-129, April 1998.

17) Tsuchiya, H., Toyooka, Y.: "Relation between SPT N-value and measured values (P_f, E_p) by pressuremeter tests", Sounding Symposium, Japanese Society of Soil Mechanics and Foundation Engineering, pp. 101-108, 1980.